Pacific Northwest
NATIONAL LABORATORY

PNNL-32446

Examining Nuisance Aerosol Detections in Light of the Origin of the Screening Process

November 2021

Harry S. Miley
Paul W. Eslinger
Judah I. Friese

U.S. DEPARTMENT OF ENERGY

Prepared for the U.S. Department of Energy
under Contract DE-AC05-76RL01830

PACIFIC NORTHWEST NATIONAL LABORATORY
operated by
BATTELLE
for the
UNITED STATES DEPARTMENT OF ENERGY
under Contract DE-AC05-76RL01830

Printed in the United States of America

Available to DOE and DOE contractors from the
Office of Scientific and Technical Information,
P.O. Box 62, Oak Ridge, TN 37831-0062;
ph: (865) 576-8401
fax: (865) 576-5728
email: reports@adonis.osti.gov

Available to the public from the National Technical Information Service
5301 Shawnee Rd., Alexandria, VA 22312
ph: (800) 553-NTIS (6847)
email: orders@ntis.gov <https://www.ntis.gov/about>
Online ordering: http://www.ntis.gov

Examining Nuisance Aerosol Detections in Light of the Origin of the Screening Process

Harry S. Miley, Paul W. Eslinger, Judah I. Friese

Executive Summary

The evolution of philosophy and computations in the International Data Center (IDC) related to aerosol samples have had profound impacts on the number of recorded detections in the network since routine operations began in 2000. Key decisions from policymakers have been the list of triggering radionuclides, the scheme for categorizing these into interest levels 1-5, and an algorithm for determining when an anthropogenic isotope is seen so often that it is no longer interesting, known as the Exponential Weighted Moving Average (EWMA). These are described in the Operations Manual of the IDC. Key parameters that are controlled by the IDC but for which the IDC receives occasional input from policymakers include the constants in EWMA and the peak significance threshold for individual gamma rays, the latter of which directly leads to determination of the presence or absence of a radionuclide in a sample. There are also changes in computations which the IDC makes and informs policy makers about, such as changes in how background is computed, which could also affect the ease of detecting a peak – real or false.

Rather than focus on the quantitative changes due to computation changes, this work records some thinking on how isotopes and peak significance levels were chosen, and the resulting detections seen over 18 years during the buildup of the International Monitoring System (IMS). These detections are considered on a global scale to try to determine the relative impact on monitoring, and in some cases, the nature of their existence. Repeated detections of ^{131}I and ^{133}I are the most troublesome, but they are not so frequent to be a major problem for the Verification Regime. These detections could probably be handled adequately using scientific methods currently under development for xenon backgrounds. It is also somewhat problematic that top-level analysis of aerosol backgrounds has not been reported previous to this.

The steep increase in the rate of detections after 2016 are a concern, either in the actual backgrounds or from changes in the calculations methods used to generate the Reviewed Radionuclide Report (RRR.) Final conclusions of the authors are that the computational stability of the RRR is very important. With computational stability, changes can be usefully analyzed as being due to changes in radioactivity in Earth’s atmosphere

This report is a distillation into text of a talk given in the Radionuclide Experts Group (RNEG) in Vienna during Working Group B (WGB) in February of 2019. This report does not directly contain any IDC data, only summaries by year, or by isotope, or by location. No specific IDC detection by time, location, or isotope is included.

History of Development

The Comprehensive Nuclear-Test-Ban Treaty [CTBT 1996] prohibits nuclear test explosions and any other nuclear explosions. The International Monitoring Systems (IMS) is the key component of the treaty verification regime and includes an 80-station aerosol radionuclide subnetwork, capable of detecting ^{140}Ba at a sensitivity of 10 μBq/m^3. The IMS is capable of detecting nuclear releases into the atmosphere of a magnitude equivalent to fission yields far below 1 kt [Werzi 2009]. The design and building of the physical aerosol network occurred in parallel with developments in the data analysis pipeline of the IDC, which after human analyst review, determines which signals are reported as detections in the Reviewed Radionuclide Report (RRR). The criteria for selecting a gamma spectrum peak as ‘present’ is crucial; it can hide a real peak from a decaying atom, or it can promote random noise into a false positive. Another key ingredient in the production of an RRR is the scheme for categorizing measurements into levels of lower to higher interest. In the late 1990s, there was no radionuclide monitoring equivalent to a seismic, infrasound, or hydroacoustic ‘event.’ A seismic event in nature is one that releases seismic energy that might be recorded by the IMS. Events are created in another arm of the

Verification Regime, the International Data Center, or IDC, to try to match these physical events when at least three stations record a tremor of sufficient size, timing, and other properties such that triangulation of the signals produces a unique event location. This process is possible because the stations are sufficiently sensitive and numerous that a 1 kt or smaller release of energy is readily detected by several stations and IDC event bulletins are generated.

Of course, there are equivalent radionuclide releases in the physical world, but the radionuclide networks (aerosol and noble gas) are not sensitive enough nor do they contain enough samplers to routinely obtain three or more measurements to establish an event tied to a well-defined location. Much work is being done to improve this, by the use of improved atmospheric transport model (ATM) calculations and advanced statistical techniques (STAT). But in 2020, no such system was in place in the IDC.

Without an IDC RN event bulletin which draws several measurements together, experts in the 1990s formulated a scheme to categorize the level of interest in a single radionuclide measurement. The categorization scheme uses a list of isotopes to trigger a shift from Levels 1 and 2 (natural radioactivity only), to Levels 3, 4, and 5, which are normal concentrations of trigger isotopes, abnormal concentrations of one trigger isotope, and abnormal concentrations of at least two trigger isotopes, respectively.

Related excerpts from WGB Documents that address the categorization scheme developed for the IMS are the following:

TL/2-10 (June 1998)

- *A "standard list of relevant fission and activation products" should be employed in the event screening decision logic. A model list for initial consideration and testing is provided…. The standard list should be revised as necessary as experience is gained with its use.*
- *The data from the particulate sensors and the noble gas sensors should be combined and considered as aggregate data in the screening process.*

TL-2/30: Aug 1999

- *Revised Standard List… has 37 isotopes*

WGB-10 (1999) Event Screening

- *WGB considered the issue of relevant fission and activation products for event screening of data from radionuclide stations. WGB discussed the relative advantages of a comprehensive list and a more selective list of radionuclides for use in automated and reviewed reports, and the generation of event bulletins. There was agreement to continue further discussion on which type of list is appropriate for these purposes. An area highlighted for further investigation is the need to minimize false identification.*

TL-2/40: Feb 2000

- *Recommended Standard List… has 84 isotopes*

WGB-11 (2000) Event Screening

- *The IDC technical expert group on event screening has recommended a revised standard list of relevant radionuclides for IDC event screening (CTBT/WGB/TL-2/40 and Corr.1). This revised list will be incorporated into the IDC Release 3 applications software for testing and development.*

WGB-23 (Sept 2004) IDC RN Data Products

- *38… WGB suggested that the IDC begin an experiment with enhanced sensitivity and report the results to the Twenty-Fourth Session of WGB, along with a schedule for release of the software to States Signatories.*

TL/2-85 (Feb 2005)

- *The adjustment of the critical limit for peak search rendered a higher number of level 4 and 5 events than expected. In the short term, the setting should be readjusted towards a nominal type I error frequency of 0.001% and should be re-evaluated when refinements to nuclide identification algorithms, background subtraction and screening criteria for event categorization are implemented.*

The nature of the provisional operations of the IMS and IDC are to build up and test the verification regime such that the regime is ready by the time the Treaty enters into force. Thus, the provisional operations period is invaluable for development purposes–the international monitoring community didn't have access to a data set of this nature before this period began.

Making Isotope Lists and Comparing Isotopes of Interest to Backgrounds

In the negotiation process, there were at least two schools of thought for how an IDC isotope list should be composed. Experiments and computations were done, but the key philosophical divide was that of a long list [Matthews 2005] versus a short list [Miley and Arthur 1999, Miley et al 2001].

The short list perspective was derived from historical data and from gamma spectroscopy experience. A calculation from first principles and a measurement of irradiated ^{235}U were used [Miley & Arthur 1999] to develop a rating (a figure of merit) for fission products based on their ability to discriminate between explosions and other uses of nuclear materials. A similar figure of merit (FOM) was developed for activation products.

A few isotopes were much more informative than all others for both fission products and activation isotopes. Gamma spectroscopy experience shows also that the longer the list of isotopes of interest, the more likely a statistical false positive is to occur.

Fission Products

Fission products are the atoms left after an actinide like ^{235}U or ^{239}Pu undergoes fission. These debris atoms are quite rich in neutrons, and so rapidly decay until they are on or near the 'line of stability.'

Considering only fission products, the left panel of Table 1 shows a combination of historical monitoring results by Lars Erik DeGeer (LEDG), a first principles calculation (CMR) done by the Center for Monitoring Research, and a PNNL experiment [Miley and Arthur 1999, Miley et al 2001]. In Figure 1, we see the figure of merit (FOM) rapidly decreasing such that much of the value for verification purposes would be derived by the first 10, or perhaps 25, fission isotopes.

The situation with respect to activation products is somewhat more complex. The neutrons emitted during a nuclear explosion can transform, or 'activate' nearby atoms, so this is a function of the environment around the device. The results can be quite different in the atmosphere, in soil, or in sea water. Because other experiments and calculations are not available, the left panel of Table 2 shows development of a figure of merit for activation products based on the same LEDG detections, plus some activation calculations for soil which is representative of underground (UG) explosions and seawater which is representative of underwater (UW) explosions. Unit penalties in the figure of merit are taken for isotopes that are frequently used in systems for calibration or which have a background interference from natural radioactivity.

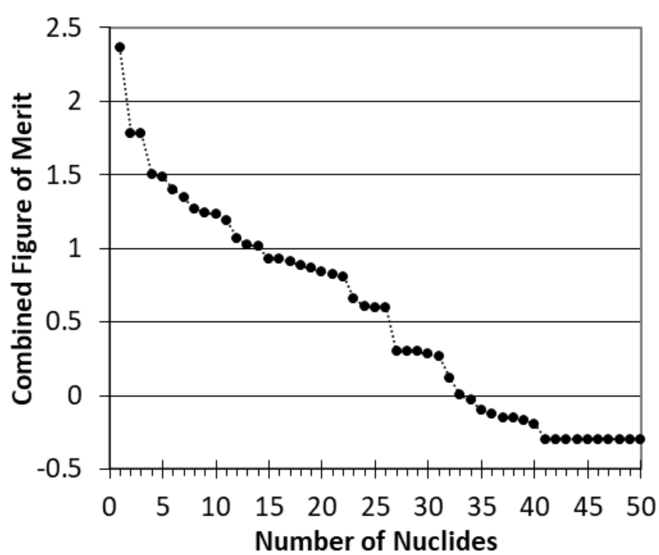

Figure 1. A figure of merit (FOM) derived from the data in Table 1 combining experimental, first principles calculations, and field data.

Table 1. A figure of merit approach for the first 33 of 54 fission products, and IMS background hits in 2012-2017.

Rank	Isotope	FOM	LEDG Detect	CMR Calc	PNNL Expt	T1/2	Fission Yield	Energy or Abund	Isotopic Interfere	Total Hits	L3	L4	L5
1	141Ce	2.36	Yes	230	1					1	0	1	0
2	140Ba	1.78	Yes	110	2					2	0	2	0
3	140La	1.78	Yes	110	2					0	0	0	0
4	95Zr	1.5	Yes	98	4					0	0	0	0
5	99Mo	1.48	Yes	22	3				Tc-99m	0	0	0	0
6	103Ru	1.4	Yes	1500						1	0	0	1
7	147Nd	1.34	Yes	36	6				I-133	1	0	1	0
8	131I	1.27	Yes	260						681	444	222	15
9	132Te	1.24	Yes	170					Te-131m	0	0	0	0
10	144Ce	1.23	Yes	5.1	5					0	0	0	0
11	133I	1.19	Yes	87		< 1 d			Nd-147	36	12	16	8
12	126Sb	1.07	Yes	17					Te-129m	0	0	0	0
13	127Sb	1.02	Yes	8.8						0	0	0	0
14	137Cs	1.02	Yes	1	9					3673	3084	522	67
15	115Cd	0.93	Yes	0.6	17		< 0.017		Ac-228	0	0	0	0
16	136Ce	0.92	Yes	0.37	11					1	0	1	0
17	105Rh	0.91	Yes	2						0	0	0	0
18	111Ag	0.88	Yes	0.31	16					0	0	0	0
19	129mTe	0.87	Yes	1.1				< 5 %	Sb-126	1	0	1	0
20	97Zr	0.84	Yes	0.15	13	< 1 d			Sb-128	0	0	0	0
21	156Eu	0.83	Yes	0.14	15				Bi-214	0	0	0	0
22	106Ru	0.81	Yes	0.49						31	11	18	2
23	99Tc	0.65		210		< 1 d			Mo-99	145	59	84	2
24	95Nb	0.61	Yes		4				Bi-214	1	0	0	1
25	155Eu	0.6	Yes	0.03						1	0	1	0
26	125Sb	0.6	Yes	0.03						0	0	0	0
27	91Y	0.3	Yes					< 1 %		0	0	0	0
28	125Sn	0.3	Yes							0	0	0	0
29	143Ce	0.3	Yes						Pb-214	0	0	0	0
30	131mTe	0.28		1.3					Te-132	0	0	0	0
31	153Sm	0.27		1.1						1	0	1	0
32	151Pm	0.11		0.14					Ac-228	0	0	0	0
33	112Pd	0		0	8	< 1 d	< 0.017			0	0	0	0

For underground explosions, several isotopes have calculated activation quantities for 1 kt of fission neutrons that are in the 10^{12}–10^{13} Bq range. However, for underwater explosions in the sea, the calculated activity for ^{24}Na is 5 orders of magnitude higher than the activity of the second-rated ^{51}Cr.

We are now prepared to consider the nominal verification utility (figure of merit) of isotopes versus their frequency of detection in the Earth's atmosphere. A high frequency of detection dilutes the power of a signature to call attention to a possible explosion.

Table 2. A figure of merit (FOM) approach for the first 22 activation products, and IMS background hits for 2012-2017.

Rank	Isotope	FOM	LEDG Detect	UG 1kt @ 10d Activity (Bq)	UW 1kt @ 10d Activity (Bq)	Calib Isotope	Bkg Interfere	Total Hits	L1	L2	L3
1	24Na	3.94	Yes	4.68E+12	4.90E+11			5614	4647	963	4
2	51Cr	3.54	Yes	9.00E+12	4.90E+06			3	0	3	0
3	122Sb	3.54	Yes	3.26E+11	9.10E+07			3	0	3	0
4	124Sb	3.51	Yes	7.58E+11	2.10E+07			0	0	0	0
5	65Zn	3.45	Yes	4.10E+11	6.60E+06			6	0	3	3
6	133Ba	3.06	Yes	1.35E+09	2.40E+04			1	0	1	0
7	134Cs	1.51		7.50E+11	1.70E+07			859	780	26	53
8	42K	1.48		3.12E+10	1.40E+08			3	0	3	0
9	46Sc	1.46		2.71E+13	1.94E+05			0	0	0	0
10	59Fe	1.42		1.38E+13	1.16E+05			10	1	7	2
11	187W	1.32		5.73E+10	1.10E+06			0	0	0	0
12	110mAg	1.23		5.46E+09	6.70E+05			0	0	0	0
13	69mZn	0.82		4.50E+07	7.34E+02			9	0	9	0
14	60Co	-0.5	Yes	3.52E+12	6.50E+06	Yes		372	251	119	2
15	54Mn	-0.6	Yes	5.71E+12	4.70E+04		Yes	29	11	16	2
16	152Eu	-0.7	Yes	1.94E+12	2.90E+04	Yes		2	0	2	0
17	196mAu	-1						0	0	0	0
18	203Pb	-1						0	0	0	0
19	47Sc	-2.3		3.80E+12	8.30E+08		Yes	1	0	1	0
20	152mEu	-2.7		1.92E+12	2.90E+04	Yes		0	0	0	0
21	132Cs	-2.8		1.13E+10	2.60E+05		Yes	0	0	0	0
22	57Co	-3	Yes			Yes		0	0	0	0

LEDG – A combination of historical monitoring results by Lars Erik DeGeer
UG – Underground explosion
UW – Underwater explosion

In the strongest form of the verification regime, each monitoring technology should be able to stand alone. However, if a radionuclide signature is detected with a magnitude consistent with historical background for that location, the radionuclide signal alone would be a very weak argument for elevating interest. Some sort of data fusion with a seismic, hydroacoustic, or infrasound signal, or perhaps other auxiliary information could raise the interest in an otherwise non-anomalous radionuclide signal.

Figure 2 shows the figure of merit for the top-rated activation and fission isotopes in the current IDC trigger list against the number of detections in the IMS in the 2012-2017 time period. In the activation isotope panel, we see that ^{24}Na was detected thousands of times in the 2012-2017 time period. Initially, one might think that the overwhelming natural background of ^{24}Na reduces the value of the isotope, but the coincidence of a release of ^{24}Na (perhaps combined with an even larger xenon gas release), which coincided with a hydroacoustic signal would be a telltale underwater signature. One might argue that the xenon isotopes could provide verification information without ^{24}Na, but there are half as many IMS xenon locations as aerosol locations, so the xenon signal might be missed.

None of these considerations include the impact of chemistry on the release of isotopes, with the possible exception of the LEGD detections. The volatility of an element at a given temperature determines whether it behaves more as a gas than a particle. Let us consider the isotopes detected near U.S. underground nuclear tests, as reported in [DOE/NV-317] and shown in Table 3. By far, the volatile iodine isotopes dominate this list, and many others have noble gas parent isotopes.

The significance of the half-life ($T_{1/2}$) of the detected isotopes is that many of these would be greatly reduced by decay before being transported the distance scale of the separation of IMS aerosol stations, 1000 km, e.g. ^{135}I at $T_{1/2}$= 6.6 h. The significance of the $T_{1/2}$ of the noble gas parent isotope is that a substantial portion of leakage must have occurred in a few parent half-lives, or the parent could be extinguished before escaping.

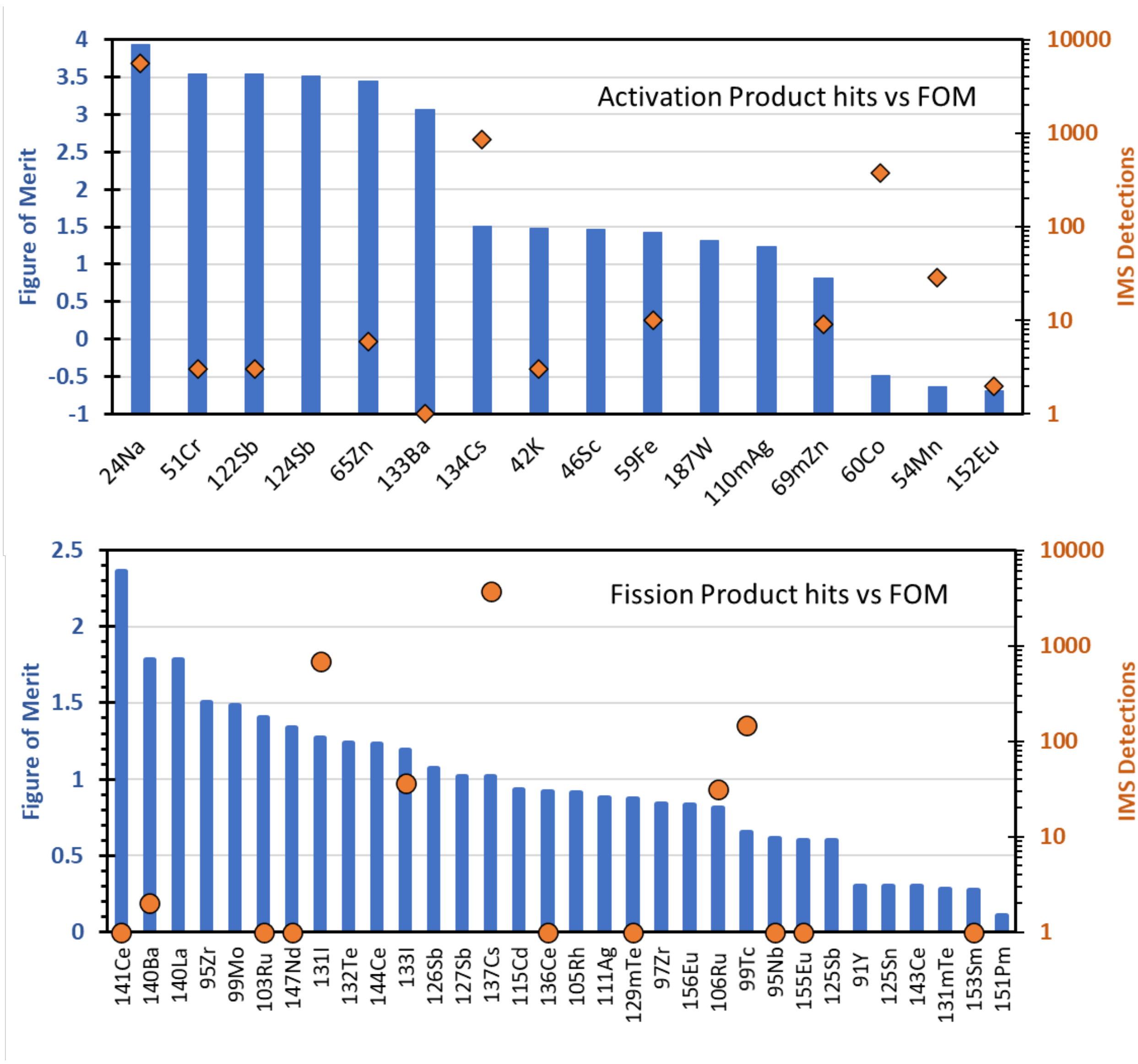

Figure 2. Figure of Merit (FOM) for activation and fission product isotopes vs background detections in the IMS in 2012-2017.

Another factor to consider in this chemical fractionation is temperature of the effluent. Iodine, cesium, and tellurium isotopes were prevalent in Fukushima effluent, which probably indicates the temperature of gases crossing through the reactor containment features were high enough for those elements to be substantially volatile.

The point of this discussion of actual releases is to again scrutinize the IMS background detections. The prevalence of ^{24}Na has been discussed, and the isotope must be relied on because of the scarcity of xenon systems. The small number of ^{140}Ba hits is only slightly worrisome, as essentially any detection of ^{140}Ba is an interesting anomaly. The detections of ^{131}I and ^{133}I are most concerning. These are presumably leaking from civilian nuclear facilities, or leakage from the use of medical isotopes.

Table 3. Isotopes observed leaking after U.S. underground explosions in Nevada, from DOE/NV-317. The presence of non-volatile isotopes on the list may occur because a noble gas precursor aided in its escape from containment.

Rank	Isotope	Frequency	T1/2		NG Parent Isotope	T1/2	
1	133I	63	20.3	h			
2	131I	62	8.04	d			
3	135I	62	6.61	h			
4	138Cs	27	32.2	m	138Xe	14.1	m
5	140Ba	19	12.8	d	140Xe	13.6	s
6	88Rb	15	17.8	m	88Kr	2.84	h
7	103Ru	14	39.4	d			
8	132Te	13	77.9	h			
9	132I	11	143	m			
10	91Sr	8	9.7	h	91Kr		
11	134I	8	52.6	m			
12	95Zr	6	64.4	d	95Kr	0.78	s
13	106Ru	5	368	d			
14	139Ba	5	84.9	m	139Xe	39.7	s
15	141Ce	5	32.4	d	141Xe	1.72	s
16	137Cs	4	30.1	y	137Xe	3.82	m

Viewing Development of the IMS Aerosol Network Through IDC Reports

As mentioned above, the IDC receives daily data from RN aerosol stations, subjects them to automated pipeline processing, and with a human analyst review, creates daily RRRs for each measurement from the station. About 269,000 such RRRs were produced from 2001 through 2018. During this time period, the number of stations in operation went from zero to almost 70.

Figure 3 shows the gradual growth of the number of RRRs and an interesting evolution of hits per year. The Total Hits is comprised of detections categorized as levels L4 and L5, plus level L3, which include one or more trigger isotopes which have been detected often enough to be considered 'normal' for that station. The number of Total Hits (L3+L4+L5) can be readily changed by adjusting the peak sensitivity of the analysis pipeline. The difference between the Total and L4+L5 is the algorithm (Exponentially Weighted Moving Average) that moves detections of isotopes into the 'normal fission or activation product' category, L3, which is not considered anomalous, although the L4 and L5 levels are.

In 2011, Fukushima reactor releases occurred, and the aerosol release, primarily of iodine, tellurium, and cesium isotopes, was perhaps the equivalent of an atmospheric test on the range of 10-50 kilotons. If we divide the number of hits for 2011 by the number of reporting stations, we obtain 140 hits per station that year. Many of these detections were three orders of magnitude above detection thresholds. This shows how the aerosol network could respond to a 0.1 kiloton surface/atmospheric test.

Besides the peak in hits in 2011, there is interesting structure, some of which can be explained by documented changes to the aerosol analysis pipeline.

Analyzing the Hits Per Year

Looking back at the years in which the Provisional Technical Secretariat (PTS) was creating the IDC processing pipeline and the IMS network presents challenges. What changes are due to the modifications in the analysis pipeline, and what changes are due to the growth of the IMS in number and in areas with new background radioactivity sources? To partially unravel the question, the hits (detections of relevant radionuclides) per station per year are shown in Figure 4. The large peak in 2011 is from samples containing radioactive debris from the Fukushima reactor accident. The other structures must be due to changes in software, differences in the region the IMS began to sample, or changes in quantity or type of radioactivity leaked to the atmosphere. These structures are not completely understood.

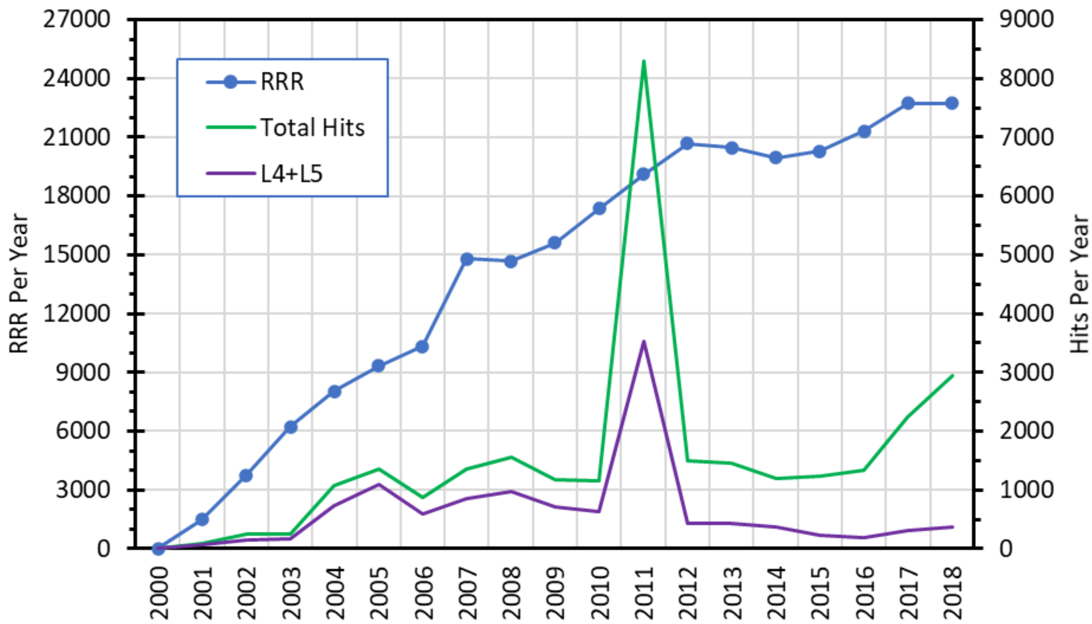

Figure 3. The growth of the number of RRRs is shown with the evolution of hits per year. Total hits are the sum of sample RRRs with levels L3, L4, and L5.

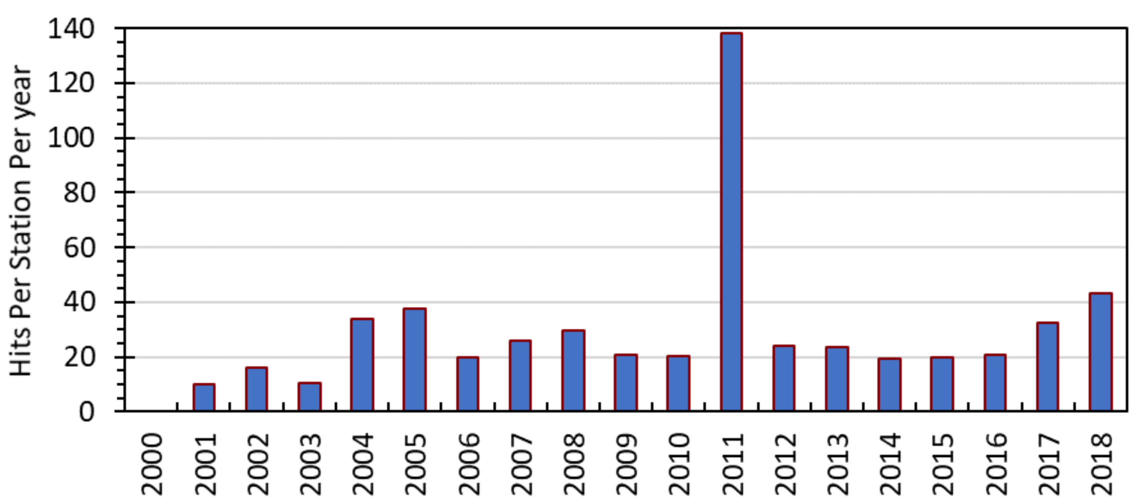

Figure 4. Detections recorded each year of any isotope on the IDC trigger list. The pronounced peak in 2011 includes the sum of all Fukushima detections.

Early Years: The early years of operation of the IDC pipeline processing and analyst review experienced on the order of 100 detects per year from the trigger list of isotopes. These detects, and their frequency per week are shown in Table 4. A more complete table is provided in Appendix I. From Figure 4, one can see the rate of hits per station is between 10 and 20. The patterns of frequent ^{137}Cs, ^{99m}Tc, and

^{131}I hits became evident. The isotope ^{99m}Tc is the decay product of ^{99}Mo, which is a valuable explosion signature but also an isotope used for cardiovascular diagnostics. In fact, because ^{99m}Tc is more readily detected than ^{99}Mo, the detection of ^{99}Mo is frequently accomplished by inferring its presence from that of its decay product.

In Table 5 we see evidence of strong change in the IDC processing parameters. A more complete table is provided in Appendix I. From Figure 4 we see that 2004 and 2005 had over 35 hits per station per year, about double the first three years. Documents from February 2004 show subject matter experts uncovered that the peak significance parameter was set to an unreasonably high value. By February 2005, experts were complaining that the significance parameter was set unreasonably low, and from 2006 to 2016, excepting the Fukushima year, the hits per station per year was close to 20. There was an unexplained rise in 2017-2018 to values similar to 2004-2005.

Considering IMS Aerosol Isotope Detections Since Fukushima

The period since Fukushima was chosen for additional study, as the data analysis pipeline has been relatively stable. Figure 4 shows this period to have about 20 hits per station per year, and Table 6 shows that ^{24}Na and ^{137}Cs account for a large share of that signal. A more complete table is provided in Appendix I. The prevalence of ^{134}Cs is interesting. Detection of ^{137}Cs, $T_{1/2} = 30.2$ y, is frequently attributed to Chernobyl resuspension or as a legacy of atmospheric nuclear explosion. For ^{134}Cs, the much shorter $T_{1/2} = 2.06$ y makes historic attributions more difficult. The more natural explanation is that this is related to the Fukushima reactor accident.

Table 4. A summary of trigger isotopes detected by the IMS aerosol stations in the first three years of regular operation, showing the year, the total hits, the categorization of the hits. Some isotopes with unexpected higher rates are highlighted.

					WGB-19									
Year				Total Hits	Change to 99mTc Cat Scheme proposed too soon									
2001				89	2002				244	2003				257
Nuclide	L3	L4	L5	avg hits/wk	Nuclide	L3	L4	L5	avg hits/wk	Nuclide	L3	L4	L5	avg hits/wk
CS-137	12	5	1	0.35	AU-198	0	0	1	0.02	CS-137	94	79	3	3.38
I-131	0	18	3	0.40	CE-141	0	1	0	0.02	I-131	0	13	2	0.29
NA-24	0	8	0	0.15	CO-58	0	0	1	0.02	K-42	0	1	0	0.02
RU-103	0	0	1	0.02	CO-60	0	1	0	0.02	NA-24	0	29	1	0.58
SB-124	0	1	0	0.02	CS-137	102	40	2	2.77	RB-84	0	1	0	0.02
TC-99M	0	35	5	0.77	I-131	0	45	6	0.98	RU-103	0	1	0	0.02
					I-133	0	0	1	0.02	TC-99M	0	29	0	0.56
					NA-24	0	7	1	0.15	ZN-65	0	3	0	0.06
					SB-122	0	1	0	0.02	ZR-97	0	1	0	0.02
					SB-124	0	0	1	0.02					
					TC-99M	0	29	4	0.63					
					ZN-65	0	0	1	0.02					

Table 5. A summary of detections by the IMS aerosol stations showing large changes due to new processing parameters.

EG Minutes:				WGB-23	TL-2/85									
Feb 2004 Why are we getting so few L5?			Begin expt w/enhanced sensitivity		Feb 2005 peak search criteria change gave high L4 & L5									
2004				1080	2005				1347	2006				865
Nuclide	L3	L4	L5	avg hits/wk	Nuclide	L3	L4	L5	avg hits/wk	Nuclide	L3	L4	L5	avg hits/wk
AG-111	0	1	0	0.02	AG-110M	0	1	0	0.02	AS-76	0	1	0	0.02
AS-76	0	1	0	0.02	AG-111	0	4	0	0.08	AU-196	0	1	0	0.02
AU-196	0	1	0	0.02	AS-76	0	7	1	0.15	AU-198	0	1	0	0.02
CD-115	0	2	0	0.04	AU-196	0	0	1	0.02	CO-58	0	1	0	0.02
CE-141	0	3	0	0.06	AU-198	0	4	1	0.10	CO-60	3	90	0	1.79
CE-144	0	0	1	0.02	CD-115	0	4	0	0.08	CS-137	82	88	0	3.27
CO-57	0	3	1	0.08	CD-115M	0	6	1	0.13	EU-155	0	1	0	0.02
CO-58	0	6	0	0.12	CE-141	0	5	0	0.10	I-131	2	33	2	0.71
CO-60	19	103	5	2.44	CE-144	0	9	0	0.17	K-42	0	4	0	0.08
CR-51	0	5	0	0.10	CO-57	0	2	0	0.04	MN-54	0	2	0	0.04
CS-132	0	2	0	0.04	CO-58	0	18	0	0.35	MO-99	0	1	0	0.02
CS-136	0	1	0	0.02	CO-60	44	157	13	4.12	NA-24	172	289	0	8.87
CS-137	339	122	7	9.00	CR-51	0	6	0	0.12	PD-112	0	2	0	0.04
I-131	0	21	2	0.44	CS-132	0	5	0	0.10	RA-224	1	5	0	0.12
I-133	0	7	2	0.17	CS-137	240	120	18	7.27	RB-84	0	1	0	0.02
I-135	0	0	1	0.02	EU-152	0	0	1	0.02	RU-103	0	3	0	0.06
IR-192	0	1	0	0.02	EU-155	0	2	0	0.04	SB-120	0	1	0	0.02
K-42	0	6	0	0.12	EU-156	0	1	0	0.02	SB-122	0	11	0	0.21
LA-140	0	1	0	0.02	FE-59	0	1	0	0.02	SB-124	0	1	0	0.02
MN-54	0	1	0	0.02	I-131	7	53	3	1.21	TC-99M	9	23	2	0.65
NA-24	19	242	8	5.17	I-133	0	28	3	0.60	TE-129M	0	1	0	0.02
PD-112	0	2	1	0.06	I-135	0	1	0	0.02	Y-88	0	3	0	0.06
PM-151	0	1	0	0.02	K-42	0	21	1	0.42	Y-91	0	9	0	0.17
RA-224	6	22	1	0.56	MN-54	0	2	1	0.06	ZN-65	0	12	0	0.23
RB-84	0	2	0	0.04	NA-24	167	278	7	8.69	ZN-69M	0	7	0	0.13
RH-102	0	1	0	0.02	NP-239	0	0	1	0.02	ZR-95	0	1	0	0.02
RU-103	0	2	0	0.04	PB-203	0	1	0	0.02					
SB-120	0	6	0	0.12	PD-112	0	13	1	0.27					
SB-122	0	16	2	0.35	PM-151	0	4	1	0.10					
SB-124	0	2	0	0.04	RA-224	2	8	1	0.21					
SB-128	0	1	0	0.02	RB-84	0	4	0	0.08					
SC-47	0	1	0	0.02	RB-86	0	2	0	0.04					
SM-153	0	1	0	0.02	RH-105	0	2	0	0.04					
TC-99M	0	43	5	0.92	RU-103	0	16	2	0.35					
Y-88	0	10	1	0.21	RU-106	0	9	1	0.19					
Y-91	0	5	1	0.12	SB-120	0	9	2	0.21					
ZN-65	0	15	0	0.29	SB-122	0	22	2	0.46					
ZN-69M	0	21	0	0.40	SB-124	0	8	0	0.15					
ZR-95	0	0	1	0.02	SB-125	0	2	0	0.04					
ZR-97	0	3	0	0.06	SC-47	0	2	0	0.04					
					SM-153	0	8	0	0.15					
					SR-91	0	2	1	0.06					
					TC-99M	14	40	5	1.13					
					TE-129M	0	2	1	0.06					
					Y-88	0	17	1	0.35					
					Y-91	0	30	3	0.63					
					Y-93	0	2	0	0.04					
					ZN-65	0	30	0	0.58					
					ZN-69M	0	53	0	1.02					
					ZR-89	0	4	0	0.08					
					ZR-97	0	2	0	0.04					

Table 6. A summary of trigger isotopes detected by the IMS aerosol stations in the years after the Fukushima reactor accident, showing the year, the total hits, the categorization of the hits. The highlights identify the isotopes with the highest detection rates.

2012				1489	2013				1451	2014				1187	2015				1237
Nuclide	L3	L4	L5	avg hits/wk	Nuclide	L3	L4	L5	avg hits/wk	Nuclide	L3	L4	L5	avg hits/wk	Nuclide	L3	L4	L5	avg hits/wk
BA-133	0	1	0	0.02	CO-60	0	10	0	0.19	CO-60	0	3	0	0.06	CO-60	0	2	0	0.04
CO-60	0	1	1	0.04	CS-134	245	6	14	5.10	CS-134	150	6	15	3.29	CS-134	96	3	3	1.96
CS-134	245	7	17	5.17	CS-137	374	97	19	9.42	CS-137	327	78	15	8.08	CS-137	380	55	4	8.44
CS-137	643	113	20	14.92	I-131	10	33	3	0.88	I-131	12	35	1	0.92	FE-59	0	0	1	0.02
EU-152	0	1	0	0.02	NA-24	386	224	2	11.77	NA-24	333	184	0	9.94	I-131	35	31	1	1.29
I-131	11	31	3	0.87	RA-224	9	6	1	0.31	RA-224	5	13	0	0.35	I-133	0	1	1	0.04
NA-24	63	195	1	4.98	SM-153	0	1	0	0.02	TC-99M	0	9	1	0.19	MN-54	0	0	1	0.02
RA-224	102	18	1	2.33	TC-99M	1	10	0	0.21						NA-24	471	99	0	10.96
TC-99M	1	14	0	0.29											NB-95	0	0	1	0.02
															RA-224	18	12	0	0.58
															TC-99M	12	10	0	0.42

In Figure 5, two models of the ^{134}Cs detections are considered, Model 1 with a 2.06 y decay from the peak number of detections observed in 2011, while Fukushima debris was still airborne, and Model 2, with a 2.06 y decay from the observed detections in 2012. Model 2 lies much closer to the experimental data.

To understand the background, it is necessary to understand where each of several isotopes were detected during those years. The frequency of detections by station for ^{134}Cs is provided in Figure 6. Similar detection location information for ^{134}Cs, ^{99m}Tc, ^{60}Co, ^{54}Mn, and ^{131}I are provided in Figures 7 through 11.

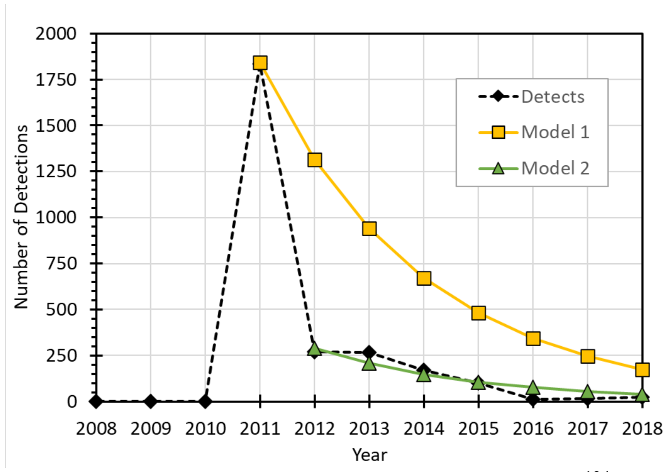

Figure 5. Different methods to explain the number of ^{134}Cs detections.

The radionuclide detectors in the IMS are sensitive enough that under favorable conditions they can detect emissions from a single patient treated medically by ^{131}I [Matthews 2009]. A further examination of that idea was performed in 2011 by the authors of this report. The prior work is included as Appendix II.

A similar finding may hold for patients treated by ^{99m}Tc. Between January 1, 2021 and September 23, 2021, there have been 11 detections of ^{99m}Tc by IMS samplers at Sacramento, California, and 4 detections at Panama City, Panama. There are no known ^{99m}Tc production sources close to these samplers. Numerous other detections of ^{99m}Tc by IMS samplers can plausibly be linked to known production facilities by using atmospheric transport models.

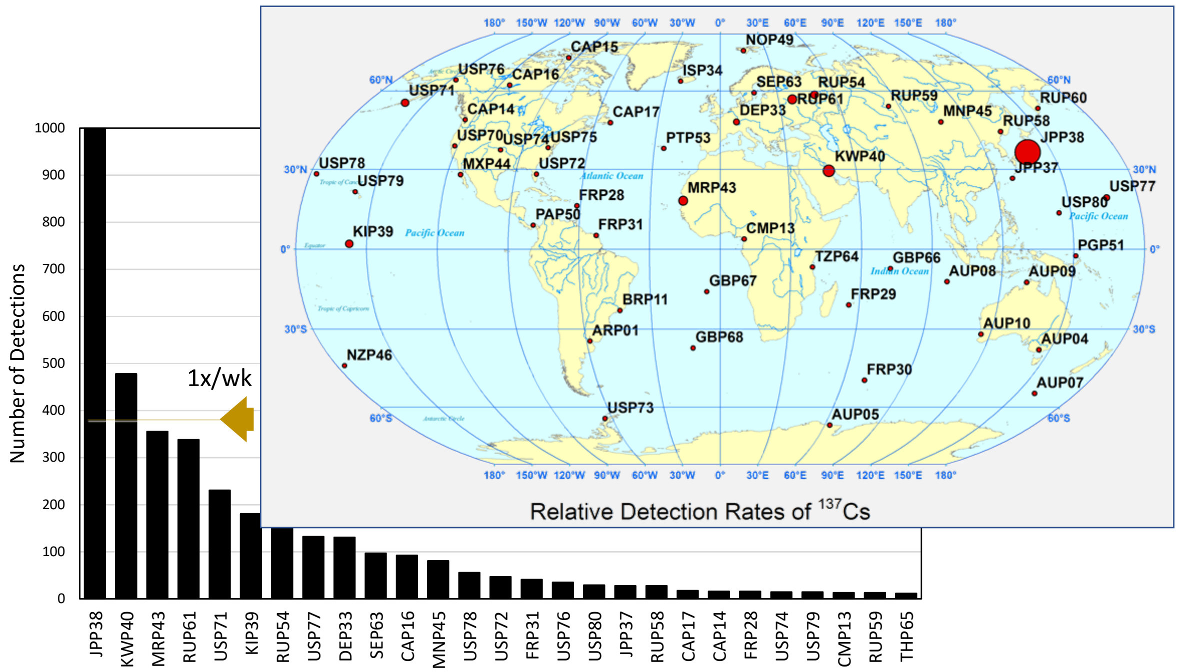

Figure 6. Global distribution of ^{137}Cs ($T_{1/2}$ = 30.2y) hits 2012-2017 with hit frequency by station. The pattern generally supports a mixed hypothesis of historic atmospheric testing (1945-1963) and debris from Chernobyl (1986) and Fukushima (2011).

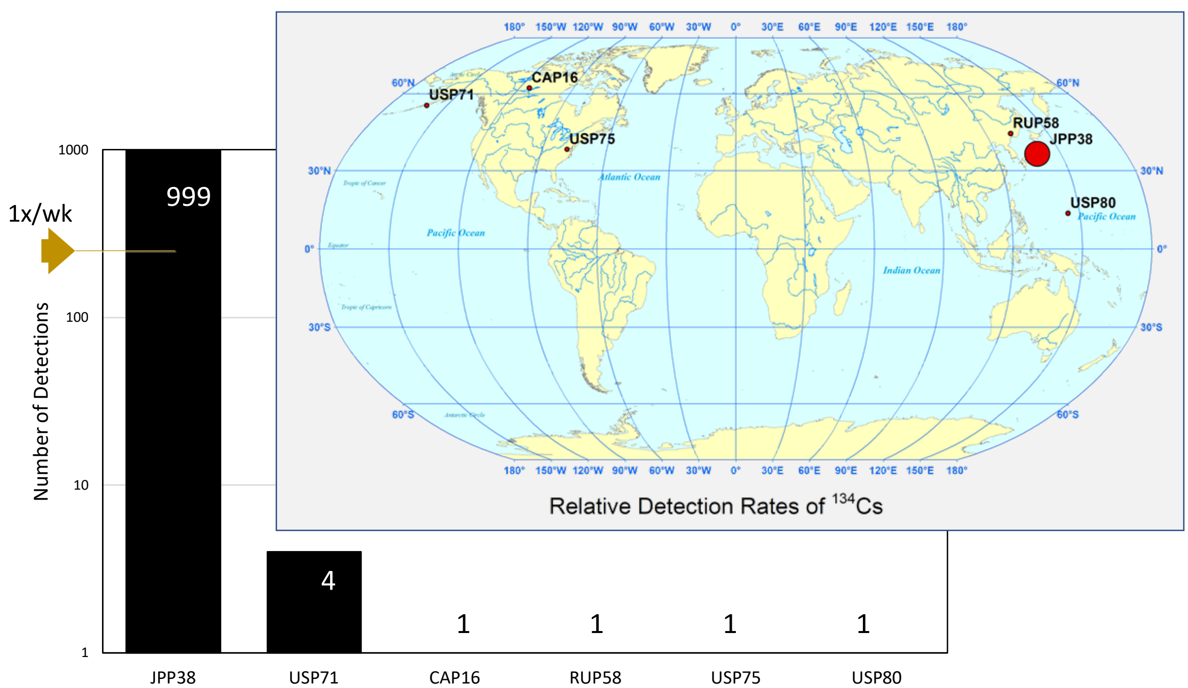

Figure 7. Global distribution of ^{134}Cs hits 2012-2017 with hit frequency by station. The ‘short’ 2-year highlife of ^{134}Cs has eliminated detectable traces from historic testing and Chernobyl, and the spatial pattern points back strongly to the Fukushima reactor accident.

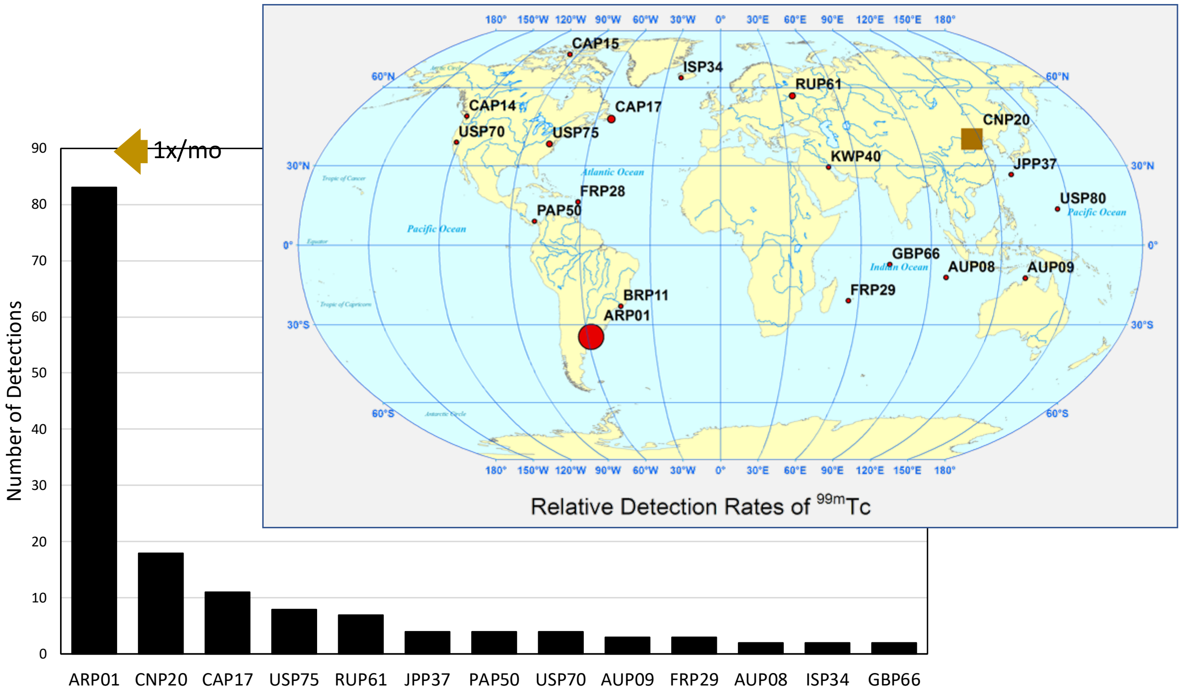

Figure 8. Global distribution of ^{99m}Tc hits 2012-2017 with hit frequency by station. A square denotes a location with a relatively high frequency on a low total number of RRRs.

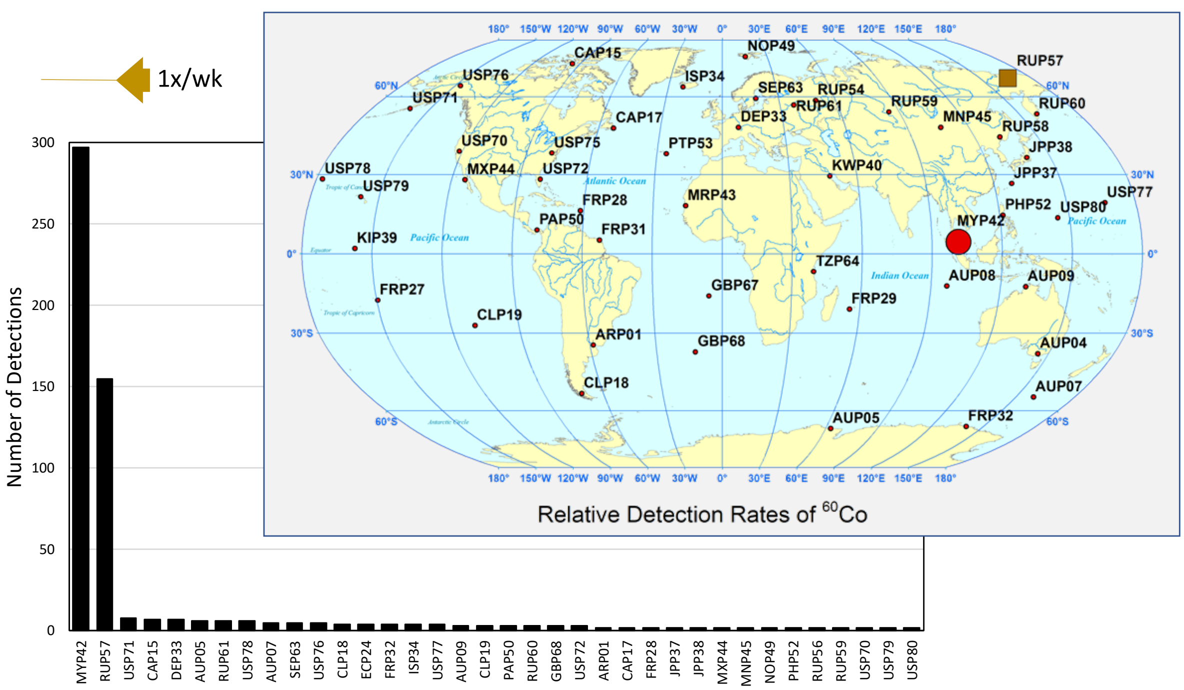

Figure 9. Global distribution of ^{60}Co hits 2012-2017 with hit frequency by station. A square denotes a location with a relatively high frequency on a low total number of RRRs. This isotope is used in the calibration of the station equipment and may not reflect radioactivity in the air.

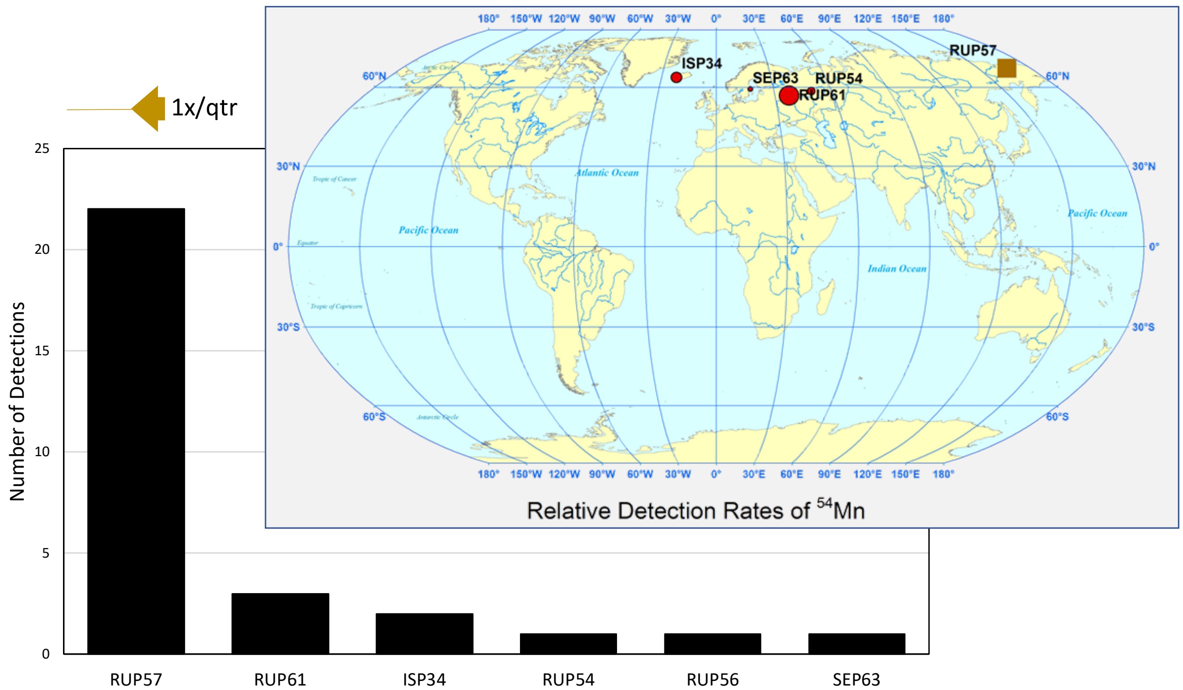

Figure 10. Global distribution of ^{54}Mn hits 2012-2017 with hit frequency by station. A square denotes a location with a relatively high frequency on a low total number of RRRs. This is an infrequent detection. One source possibility is the discharge of liquid wastes from nuclear facilities [Makhon'ko 1998].

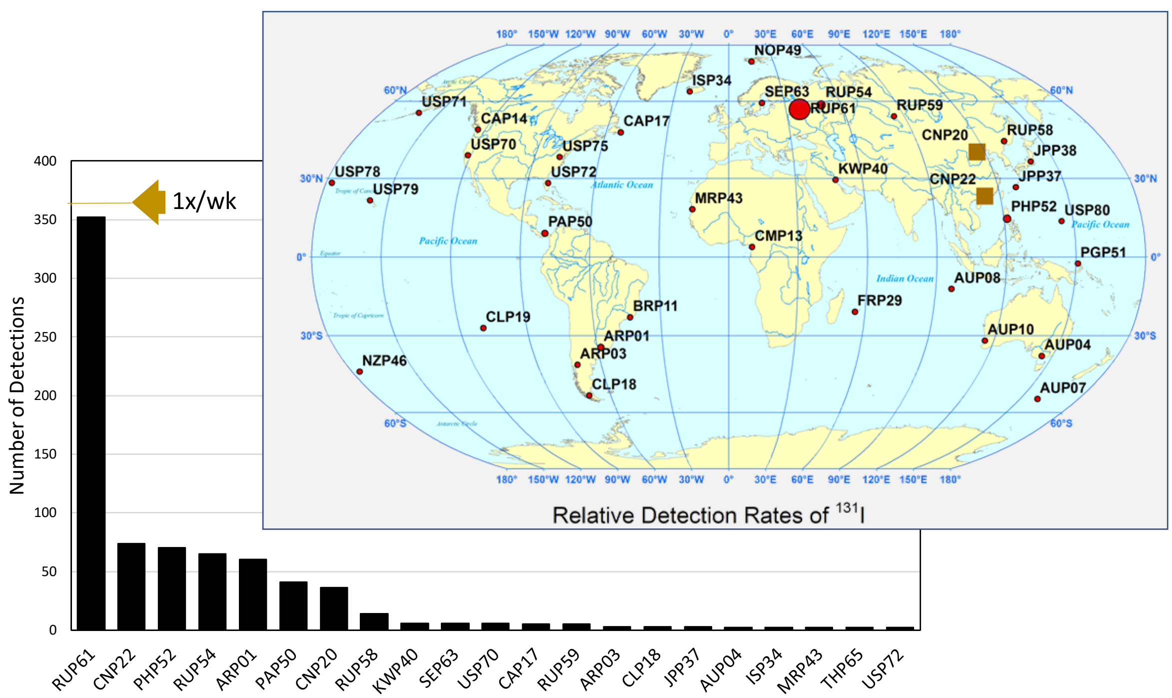

Figure 11. Global distribution of ^{131}I hits 2012-2017 with hit frequency by station. A square denotes a location with a relatively high frequency on a low total number of RRRs. Because of the importance of ^{131}I as a monitoring signature, this is one of the three most important background isotopes (together with ^{140}Ba and ^{133}I).

Observations and Conclusions

Because there is statistical noise and barely detected natural radioactivity peaks, the number of RRR isotopes detected and their frequency over a time period is quite dependent on the peak significance value. Some of the historical variation is due to adjustments to this value.

The isotope ^{24}Na has the most detections. It is detected more frequently at high north and south latitudes, which may be due to cosmic ray interactions with the Earth's magnetic field or the behavior of the layers of the atmosphere at those latitudes, or both. Because this isotope is expected to be anomalously large in debris lofted from an underwater test explosion and trivially fuse with hydroacoustic detections, these nuisance detections are not considered a serious problem.

Nuisance detections of the background ^{140}Ba is troublesome because it is the decay product of ^{140}Xe, ($T_{1/2}$ = 13.6 s) and could thus allow very sensitive aerosol detection of promptly vented underground nuclear test explosions, on the range 1-10 µBq/m^3, compared to 50-200 µBq/m^3 for IMS xenon systems.

The frequent detections of iodine isotopes ^{131}I and ^{133}I are also troubling, because of the high volatility of iodine. These isotopes are seen in the Nevada leak data to be the mostly likely aerosols to be detected. Seven stations account for most of the ^{131}I, but RUP61 (Dubna, Russia) stands out. It is a few hundred km from a medical isotope producer, which is presumed to be the source.

The detection of ^{137}Cs is usually thought of as legacy debris from nuclear testing, and resuspension of material from Chernobyl. It would be much more interesting when paired with detection of ^{134}Cs such that the clock created by the ratio matches a seismic trigger time, raising interest in both types of detection.

The isotope ^{99m}Tc suffers from fairly frequent detection in some places for medical reasons. On its own, ^{99m}Tc is not a fission product highly rated for verification value. But because it is the normal detection method for ^{99}Mo, a very highly rated explosion signature, nuisance detections of ^{99m}Tc are of concern.

In another way, the steep increase in the rate of any hits from 2017 and 2018 shown in Figure 4 are a concern, either in the actual backgrounds or from changes in the calculation methods used to generate the RRR.

Final conclusions of the authors are that the computational stability of the RRR is very important. If the algorithms are steady, changes become much more interesting, and the system history becomes an invaluable tool in interpreting new detections. A lengthy historical analysis is far more useful than a simple numerical tool for determining whether a detection is anomalous.

References

[CTBT 1996] Comprehensive Nuclear-Test-Ban Treaty. 1996. Text of the Comprehensive Nuclear-Test-Ban Treaty. United Nations Office for Disarmament Affairs (UNODA), Status of Multilateral Arms Regulation and Disarmament Agreements, CTBT. Accessed on September 20, 2012, at http://www.ctbto.org/the-treaty/treaty-text/

[DOE/NV-317] Schoengold, CR, ME DeMarre, and EM Kirkwood. 1996. Radiological Effluents Released from U.S. Continental Tests 1961 through 1992, DOE/NV-317 (Rev. 1), Bechtel Nevada, Las Vegas, Nevada. at https://www.nnss.gov/docs/docs_LibraryPublications/DOENV_317.pdf

[Makhon'ko 1998] Makhon'ko, KP, AT Korsakov, and ZA Mazurina. 1998. "Dynamics of Radioactive Contamination of the Atmosphere in the Russian Sector of the Arctic, 1954–1997." *Atomic Energy* 85(6):892-899. https://doi.org/10.1007/bf02361120

[Matthews 2009] Matthews, K.M., 2009. Spurious Iodine-131 detections at remote IMS radionuclide stations (Poster RN-06/D), ISS09 (International Scientific Studies) Conference, June 10-12, 2009. CTBTO Preparatory Commission, Vienna, Austria, http://www.ctbto.org/fileadmin/user_upload/ISS_2009/Poster/RN-06D%20%28New%20Zealand%29%20-%20Murray_Matthews.pdf

[Miley and Arthur 1999] PNNL-12194 "PNNL Review of Proposed Relevant Radionuclide List". doi:10.2172/6665. https://www.osti.gov/servlets/purl/6665

[Miley et al 2001] Miley, H. S., RJ Arthur, EA Lepel, SL Pratt, CW Thomas, Evaluation of fission product isotopes for field or laboratory detection. J of Radioanal Nuclear Chemistry 248, 651–656 (2001). https://doi.org/10.1023/A:1010628325496

[Matthews 2005] Matthews, K.M., 2005. The CTBT verification significance of particulate radionuclides detected by the International Monitoring System, 2005/1, National Radiation Laboratory, Ministry of Health, PO Box 25099, Christchurch, New Zealand, http://www.moh.govt.nz/notebook/nbbooks.nsf/0/856377d65427ad6fcc257346006f47e0/$FILE/2005-1.pdf

[Werzi 2009] Werzi, R., 2009. The operational status of the IMS radionuclide particulate network. *J Radioanal Nucl Chem* 282(3), 749. https://doi.org/10.1007/s10967-009-0270-9

ATM: Example recent ATM works

- P Eslinger et al, International challenge to predict the impact of radioxenon releases from medical isotope production on a comprehensive nuclear test ban treaty sampling station, JER, Volume 157, 2016, Pages 41-51, ISSN 0265-931X, https://doi.org/10.1016/j.jenvrad.2016.03.001
- C Maurer et al, International challenge to model the long-range transport of radioxenon released from medical isotope production to six Comprehensive Nuclear-Test-Ban Treaty monitoring stations, JER, Volume 192, 2018, Pages 667-686, ISSN 0265-931X, https://doi.org/10.1016/j.jenvrad.2018.01.030.
- P. De Meutter et al, Time resolution requirements for civilian radioxenon emission data for the CTBT verification regime, JER, Volume 182, 2018, Pages 117-127, ISSN 0265-931X, https://doi.org/10.1016/j.jenvrad.2017.11.027.
- Delcloo A., De Meutter P. (2020) Quantification of Uncertainty in Lagrangian Dispersion Modelling, Using ECMWF's New ERA5 Ensemble. In: Mensink C., Gong W., Hakami A. (eds) Air Pollution Modeling and its Application XXVI. ITM 2018. Springer Proceedings in Complexity. Springer, Cham. https://doi.org/10.1007/978-3-030-22055-6_54

STAT: Example recent STAT developments

- D. Lucas, et al, Bayesian inverse modeling of the atmospheric transport and emissions of a controlled tracer release from a nuclear power plant, Atmos. Chem. Phys., 17, 13521–13543, 2017 https://doi.org/10.5194/acp-17-13521-2017
- Pieter De Meutter, Ian Hoffman, Bayesian source reconstruction of an anomalous Selenium-75 release at a nuclear research institute, JER, Volume 218, 2020, 106225, ISSN 0265-931X, https://doi.org/10.1016/j.jenvrad.2020.106225
- P. Eslinger, et al, Source term estimation in the presence of nuisance signals, JER, Volume 203, 2019, Pages 220-225, ISSN 0265-931X, https://doi.org/10.1016/j.jenvrad.2019.03.022
- De Meutter, et al. *et al.* Source localisation and its uncertainty quantification after the third DPRK nuclear test. *Sci Rep* **8,** 10155 (2018). https://doi.org/10.1038/s41598-018-28403-z
- Eslinger, P.W., Schrom, B.T. Multi-detection events, probability density functions, and reduced location area. J Radioanal Nucl Chem 307, 1599–1605 (2016). https://doi.org/10.1007/s10967-015-4339-3

- Tichý, O. et al. Bayesian inverse modeling and source location of an unintended ^{131}I release in Europe in the fall of 2011. Atmospheric Chemistry and Physics 17, 12677–12696 (2017) https://doi.org/10.5194/acp-17-12677-2017
- P. Eslinger, et al, Source term estimation using multiple xenon isotopes in atmospheric samples, JER, Volume 204, 2019, Pages 111-116, ISSN 0265-931X, https://doi.org/10.1016/j.jenvrad.2019.04.004

Appendix I, Table A: Complete list of detections by isotope vs year for 2001–2006.

Year: 2001 — Total Hits: 89

Nuclide	L3	L4	L5	avg hits/wk
CS-137	12	5	1	0.35
I-131	0	18	3	0.40
NA-24	0	8	0	0.15
RU-103	0	0	1	0.02
SB-124	0	1	0	0.02
TC-99M	0	35	5	0.77

2002 — 244 (WGB-19: Change to 99mTc Cat Scheme proposed too soon)

Nuclide	L3	L4	L5	avg hits/wk
AU-198	0	0	1	0.02
CE-141	0	1	0	0.02
CO-58	0	0	1	0.02
CO-60	0	1	0	0.02
CS-137	102	40	2	2.77
I-131	0	45	6	0.98
I-133	0	0	1	0.02
NA-24	0	7	1	0.15
SB-122	0	1	0	0.02
SB-124	0	0	1	0.02
TC-99M	0	29	4	0.63
ZN-65	0	0	1	0.02

2003 — 257

Nuclide	L3	L4	L5	avg hits/wk
CS-137	94	79	3	3.38
I-131	0	13	2	0.29
K-42	0	1	0	0.02
NA-24	0	29	1	0.58
RB-84	0	1	0	0.02
RU-103	0	1	0	0.02
TC-99M	0	29	0	0.56
ZN-65	0	3	0	0.06
ZR-97	0	1	0	0.02

2004 — 1080 (EG Minutes: Feb 2004 Why are we getting so few L5? / WGB-23: Begin expt w/enhanced sensitivity)

Nuclide	L3	L4	L5	avg hits/wk
AG-111	0	1	0	0.02
AS-76	0	1	0	0.02
AU-196	0	1	0	0.02
CD-115	0	2	0	0.04
CE-141	0	3	0	0.06
CE-144	0	0	1	0.02
CO-57	0	3	1	0.08
CO-58	0	6	0	0.12
CO-60	19	103	5	2.44
CR-51	0	5	0	0.10
CS-132	0	2	0	0.04
CS-136	0	1	0	0.02
CS-137	339	122	7	9.00
I-131	0	21	2	0.44
I-133	0	7	2	0.17
I-135	0	0	1	0.02
IR-192	0	1	0	0.02
K-42	0	6	0	0.12
LA-140	0	1	0	0.02
MN-54	0	1	0	0.02
NA-24	19	242	8	5.17
PD-112	0	2	1	0.06
PM-151	0	1	0	0.02
RA-224	6	22	1	0.56
RB-84	0	2	0	0.04
RH-102	0	1	0	0.02
RU-103	0	2	0	0.04
SB-120	0	6	0	0.12
SB-122	0	16	2	0.35
SB-124	0	2	0	0.04
SB-128	0	1	0	0.02
SC-47	0	1	0	0.02
SM-153	0	1	0	0.02
TC-99M	0	43	5	0.92
Y-88	0	10	1	0.21
Y-91	0	5	1	0.12
ZN-65	0	15	0	0.29
ZN-69M	0	21	0	0.40
ZR-95	0	0	1	0.02
ZR-97	0	3	0	0.06

2005 — 1347 (TL-2/85: Feb 2005 peak search criteria change gave high L4 & L5)

Nuclide	L3	L4	L5	avg hits/wk
AG-110M	0	1	0	0.02
AG-111	0	4	0	0.08
AS-76	0	7	1	0.15
AU-196	0	0	1	0.02
AU-198	0	4	1	0.10
CD-115	0	4	0	0.08
CD-115M	0	6	1	0.13
CE-141	0	5	0	0.10
CE-144	0	9	0	0.17
CO-57	0	2	0	0.04
CO-58	0	18	0	0.35
CO-60	44	157	13	4.12
CR-51	0	6	0	0.12
CS-132	0	5	0	0.10
CS-137	240	120	18	7.27
EU-152	0	0	1	0.02
EU-155	0	2	0	0.04
EU-156	0	1	0	0.02
FE-59	0	1	0	0.02
I-131	7	53	3	1.21
I-133	0	28	3	0.60
I-135	0	1	0	0.02
K-42	0	21	1	0.42
MN-54	0	2	1	0.06
NA-24	167	278	7	8.69
NP-239	0	0	1	0.02
PB-203	0	1	0	0.02
PD-112	0	13	1	0.27
PM-151	0	4	1	0.10
RA-224	2	8	1	0.21
RB-84	0	4	0	0.08
RB-86	0	2	0	0.04
RH-105	0	2	0	0.04
RU-103	0	16	2	0.35
RU-106	0	9	1	0.19
SB-120	0	9	2	0.21
SB-122	0	22	2	0.46
SB-124	0	8	0	0.15
SB-125	0	2	0	0.04
SC-47	0	2	0	0.04
SM-153	0	8	0	0.15
SR-91	0	2	1	0.06
TC-99M	14	40	5	1.13
TE-129M	0	2	1	0.06
Y-88	0	17	1	0.35
Y-91	0	30	3	0.63
Y-93	0	2	0	0.04
ZN-65	0	30	0	0.58
ZN-69M	0	53	0	1.02
ZR-89	0	4	0	0.08
ZR-97	0	2	0	0.04

2006 — 865

Nuclide	L3	L4	L5	avg hits/wk
AS-76	0	1	0	0.02
AU-196	0	1	0	0.02
AU-198	0	1	0	0.02
CO-58	0	1	0	0.02
CO-60	3	90	0	1.79
CS-137	82	88	0	3.27
EU-155	0	1	0	0.02
I-131	2	33	2	0.71
K-42	0	4	0	0.08
MN-54	0	2	0	0.04
MO-99	0	1	0	0.02
NA-24	172	289	0	8.87
PD-112	0	2	0	0.04
RA-224	1	5	0	0.12
RB-84	0	1	0	0.02
RU-103	0	3	0	0.06
SB-120	0	1	0	0.02
SB-122	0	11	0	0.21
SB-124	0	1	0	0.02
TC-99M	9	23	2	0.65
TE-129M	0	1	0	0.02
Y-88	0	3	0	0.06
Y-91	0	9	0	0.17
ZN-65	0	12	0	0.23
ZN-69M	0	7	0	0.13
ZR-95	0	1	0	0.02

Appendix I, Table B: Complete list of detections by isotope vs year for 2007–2012.

March 2011 Fukushima

2007				1357
Nuclide	L3	L4	L5	avg hits/wk
AS-74	0	1	0	0.02
AS-76	0	3	0	0.06
AU-196	0	0	1	0.02
AU-198	0	2	0	0.04
BA-133	0	0	1	0.02
CD-115	0	1	0	0.02
CD-115M	0	2	0	0.04
CE-144	0	0	1	0.02
CO-57	0	1	0	0.02
CO-58	0	1	0	0.02
CO-60	7	154	2	3.13
CR-51	0	1	0	0.02
CS-134	0	0	1	0.02
CS-137	208	114	1	6.21
EU-152	0	0	1	0.02
EU-155	0	1	0	0.02
I-131	8	32	0	0.77
I-133	0	5	0	0.10
LA-140	0	1	0	0.02
MN-54	0	18	0	0.35
MO-99	0	0	1	0.02
NA-24	267	402	1	12.88
NB-95	0	0	1	0.02
PD-112	0	2	0	0.04
RA-224	2	2	0	0.08
RU-103	0	1	0	0.02
SB-120	0	1	0	0.02
SB-122	0	16	0	0.31
SB-125	0	0	1	0.02
SC-46	0	1	0	0.02
TC-99M	14	44	3	1.17
TE-129M	0	2	0	0.04
TE-132	0	1	0	0.02
Y-88	0	5	0	0.10
Y-91	0	8	0	0.15
ZN-65	0	12	0	0.23
ZN-69M	0	2	0	0.04

2008				1565
Nuclide	L3	L4	L5	avg hits/wk
AS-76	0	3	0	0.06
AU-198	0	2	0	0.04
CD-115M	0	3	0	0.06
CE-144	0	1	0	0.02
CO-58	0	4	0	0.08
CO-60	10	166	3	3.44
CR-51	0	4	0	0.08
CS-136	0	1	0	0.02
CS-137	296	138	6	8.46
I-131	4	50	6	1.15
I-133	0	2	0	0.04
K-42	0	2	0	0.04
MN-54	0	7	0	0.13
NA-24	257	444	1	13.50
NB-95	0	3	1	0.08
PD-112	0	5	0	0.10
RA-224	4	5	0	0.17
RB-84	0	2	0	0.04
RB-86	0	0	1	0.02
RU-103	0	2	0	0.04
SB-120	0	1	0	0.02
SB-122	0	20	0	0.38
SB-124	0	1	0	0.02
SM-153	0	1	0	0.02
TC-99M	25	46	2	1.40
TE-129M	0	2	0	0.04
Y-88	0	12	0	0.23
Y-91	0	12	0	0.23
ZN-65	0	3	0	0.06
ZN-69M	0	4	0	0.08
ZR-95	0	1	1	0.04
ZR-97	0	1	0	0.02

2009				1177
Nuclide	L3	L4	L5	avg hits/wk
AG-110M	0	2	0	0.04
CE-144	0	1	0	0.02
CO-60	14	86	2	1.96
CS-137	137	146	5	5.54
FE-59	0	1	0	0.02
I-130	0	1	0	0.02
I-131	29	40	0	1.33
I-133	0	2	0	0.04
K-42	0	1	0	0.02
MN-54	0	2	0	0.04
NA-24	279	370	3	12.54
RA-224	3	5	0	0.15
RU-103	0	1	0	0.02
SB-120	0	1	0	0.02
SB-122	0	17	0	0.33
SB-124	0	1	0	0.02
TC-99M	3	22	0	0.48
Y-93	0	1	0	0.02
ZR-89	0	1	0	0.02
ZR-97	0	1	0	0.02

2010				1147
Nuclide	L3	L4	L5	avg hits/wk
BA-140	0	0	8	0.15
CO-57	0	1	0	0.02
CO-60	35	77	0	2.15
CS-137	219	137	1	6.87
EU-155	0	0	1	0.02
I-131	5	36	2	0.83
I-133	0	1	0	0.02
LA-140	0	3	8	0.21
NA-24	254	311	1	10.88
RA-224	6	2	0	0.15
SB-122	0	16	0	0.31
SM-153	0	2	0	0.04
TC-99M	0	10	3	0.25
TE-129M	0	1	0	0.02
ZN-65	0	7	0	0.13

2011				8302
Nuclide	L3	L4	L5	avg hits/wk
AG-110M	30	11	21	1.19
AG-111	0	0	1	0.02
BA-140	8	6	22	0.69
CO-60	3	23	4	0.58
CS-134	1252	147	435	35.27
CS-136	235	59	293	11.29
CS-137	1589	244	445	43.81
I-130	0	0	4	0.08
I-131	1086	227	426	33.44
I-133	0	0	27	0.52
I-135	0	0	1	0.02
LA-140	31	17	73	2.33
MO-99	0	0	6	0.12
NA-24	94	210	11	6.06
NB-95	23	16	24	1.21
PB-203	0	0	3	0.06
PM-151	0	0	1	0.02
RA-224	69	17	3	1.71
RU-103	0	2	1	0.06
SB-122	0	4	2	0.12
SB-125	4	6	8	0.35
TC-99M	6	25	38	1.33
TE-129M	241	52	243	10.31
TE-131M	0	1	2	0.06
TE-132	96	32	340	9.00
ZN-65	0	0	1	0.02
ZR-95	0	1	0	0.02

2012				1489
Nuclide	L3	L4	L5	avg hits/wk
BA-133	0	1	0	0.02
CO-60	0	1	1	0.04
CS-134	245	7	17	5.17
CS-137	643	113	20	14.92
EU-152	0	1	0	0.02
I-131	11	31	3	0.87
NA-24	63	195	1	4.98
RA-224	102	18	1	2.33
TC-99M	1	14	0	0.29

Appendix I, Table C. Complete list of detections by isotope vs year for 2013–2018.

2013				1451
Nuclide	L3	L4	L5	avg hits/wk
CO-60	0	10	0	0.19
CS-134	245	6	14	5.10
CS-137	374	97	19	9.42
I-131	10	33	3	0.88
NA-24	386	224	2	11.77
RA-224	9	6	1	0.31
SM-153	0	1	0	0.02
TC-99M	1	10	0	0.21

2014				1187
Nuclide	L3	L4	L5	avg hits/wk
CO-60	0	3	0	0.06
CS-134	150	6	15	3.29
CS-137	327	78	15	8.08
I-131	12	35	1	0.92
NA-24	333	184	0	9.94
RA-224	5	13	0	0.35
TC-99M	0	9	1	0.19

2015				1237
Nuclide	L3	L4	L5	avg hits/wk
CO-60	0	2	0	0.04
CS-134	96	3	3	1.96
CS-137	380	55	4	8.44
FE-59	0	0	1	0.02
I-131	35	31	1	1.29
I-133	0	1	1	0.04
MN-54	0	0	1	0.02
NA-24	471	99	0	10.96
NB-95	0	0	1	0.02
RA-224	18	12	0	0.58
TC-99M	12	10	0	0.42

2016				1325
Nuclide	L3	L4	L5	avg hits/wk
BA-140	0	1	0	0.02
CO-60	0	5	0	0.10
CS-134	11	1	1	0.25
CS-137	296	37	2	6.44
FE-59	0	1	0	0.02
I-130	0	1	0	0.02
I-131	91	12	2	2.02
I-133	1	6	2	0.17
K-42	0	1	0	0.02
NA-24	705	89	0	15.27
RA-224	31	6	0	0.71
TC-99M	16	4	1	0.40
ZN-65	0	0	2	0.04

2017				2246
Nuclide	L3	L4	L5	avg hits/wk
CE-141	0	1	0	0.02
CO-60	30	37	0	1.29
CS-134	15	0	0	0.29
CS-137	445	62	1	9.77
EU-152	0	1	0	0.02
I-130	0	4	0	0.08
I-131	182	50	0	4.46
I-133	5	4	1	0.19
IR-192	0	2	0	0.04
K-42	0	1	0	0.02
MN-54	4	5	0	0.17
NA-24	1167	80	1	24.00
RA-224	68	8	0	1.46
	0	0	1	0.02
	11	17	2	0.58
	0	2	0	0.04
	16	21	0	0.71
	0	2	0	0.04

2018				2941
Nuclide	L3	L4	L5	avg hits/wk
BA-140	0	1	0	0.02
CO-58	0	3	0	0.06
CO-60	221	61	1	5.44
CR-51	0	3	0	0.06
CS-134	18	3	3	0.46
CS-136	0	1	0	0.02
CS-137	619	80	6	13.56
EU-155	0	1	0	0.02
FE-59	1	6	1	0.15
GA-72	0	1	0	0.02
I-130	0	1	0	0.02
I-131	103	30	5	2.65
I-133	6	5	4	0.29
K-42	0	1	0	0.02
MN-54	7	11	1	0.37
NA-24	1522	92	0	31.04
ND-147	0	1	0	0.02
RA-224	67	9	0	1.46
RB-84	0	3	0	0.06
RB-86	0	1	0	0.02
RU-106	0	1	0	0.02
SB-122	0	1	0	0.02
SC-47	0	1	0	0.02
TC-99M	13	16	0	0.56
TE-129M	0	1	0	0.02
ZN-65	0	3	1	0.08
ZN-69M	0	3	0	0.06
ZR-89	0	1	1	0.04

Appendix II. Historical ^{131}I Study

IMS Samplers can Detect Releases from Individual Thyroid Cancer Patients Treated with ^{131}I

Paul W. Eslinger, Judah I. Friese, Harry S. Miley

April 25, 2011

Abstract

Some previously unexplained ^{131}I detections in the IMS system noted by (Matthews, 2009) may be the result of medical treatment given to single individuals, or to a few individuals. The activity administered to a patient for treatment of benign or cancerous thyroid conditions ranges from 0.2 to 10 GBq of ^{131}I. Some published studies indicate that as much as 120 MBq of the administered ^{131}I can volatilize in the first day after treatment for a patient receiving a 10 GBq treatment. Example ATM calculations using archived meteorological data and hypothetical patients at a U.S. hospital with a nuclear medicine unit indicates that, under the correct conditions, 24-hr average concentrations as distant as 100 km would be detectable with a sampler having a minimum detectable concentration of 3.0 μBq/m^3.

Background

The Comprehensive Nuclear-Test-Ban Treaty (CTBT) was adopted by the United Nations General Assembly on September 10, 1996 (CTBT, 1996). The CTBT bans all States Parties (countries ratifying the treaty) from carrying out nuclear explosions. Within the CTBT the International Monitoring System (IMS) was defined to monitor the world for nuclear Explosions (CTBTO, 2011). The IMS contains four primary monitoring technologies: radionuclide, seismic, hydroacoustic, and infrasound. A number of radionuclides detectable by equipment deployed by the IMS are produced for pharmaceutical purposes as well as being produced by nuclear explosions. Understanding the occurrence of detections of ^{131}I associated with radiopharmaceuticals is important when trying to determine whether a potentially small nuclear explosion has occurred.

The CTBT identifies 80 radionuclide stations and 79 radionuclide sampling locations around the globe. Not all stations are yet active. Since the start of 2011, radionuclide sampling data have been received from 61 different stations. However, on average, only 54 stations provide data on any given day. From 2005 through early 2010 there were 208 ^{131}I detections at 40 separate IMS sampling stations associated with level 4 or level 5 events. Detections of ^{131}I have continued at about the same rate since then. One anomaly is the large number of ^{131}I detections associated with releases from the Fukushima Dai-ichi reactors following the earthquake and tsunami in April, 2011 (Biegalski et al., 2012). None of these detections of ^{131}I are believed to be associated with releases from a nuclear explosion.

Some detections of ^{131}I have occurred near medical isotope production facilities (CNEA, 2012; JINR, 2012; NRU, 2012). Others, such as wide-spread detections across Europe in November, 2011, (IAEA, 2011) are also associated with the distribution of radiopharmaceuticals. However, some of the detections are not readily explainable by the large-scale production and distribution of radiopharmaceuticals. This disparity has been noted by others (Matthews, 2009).

Data

Iodine-131 is used in the treatment of hyperthyroidism and thyroid cancer. Activities used for treatment of hyperthyroidism ranges from 0.2 to 0.5 GBq per treatment (Matthews et al., 2010) while treatments for thyroid cancer are in the range of 1 to 10 GBq per treatment (Abu-Khaled et al., 2009; Li et al., 2012; Matthews et al., 2010). Information on the total amount of ^{131}I used for treating thyroid cancer is difficult to obtain, but the estimated use in 2009 in the United States is 1.7×10^5 GBq (Matthews et al., 2010).

Iodine-131 begins to volatilize from a patient once they receive the treatment. The toxological profile for iodine prepared by the U.S. Agency for Toxic Substances and Disease Registry (Risher et al., 2004) reviews an extensive literature based on this issue. Experiments performed in Germany (Gründel et al., 2008) evaluated the rate, as a function of the amount administered, that ^{131}I is exhaled and excreted in urine for a number of patients. Their experiments indicate that exhaled air contained about 4×10^{-5} Bq/m^3 per Bq applied on the first day after treatment, and the amount lost in exhaled air for later days follows an exponential decrease. The exhaled activity is mostly organic iodine (around 90-95% on the first few days after treatment), some atomic iodine (4-10% on the first couple of days), and the remainder is aerosol borne iodine (1-2% over the first five days). Assuming that an adult breathes about 20 m^3 of air in a day, this exhalation rate results in a release of about 8 MBq in the first day from a 10 GBq treatment. Later experiments using rats (Li et al., 2012) indicate that 0.17% of the applied ^{131}I can volatilize within 4 days. As expected, the volatilization rate decreases with time after the treatment. However, about 0.12% of the applied amount volatilized in the first 24 hours after the treatment was administered. These experiments measured total volatilization of ^{131}I from the animal, and exhaled air was only one component of the volatilization. If the same total volatilization rate applies to a human, this would indicate a release of about 120 MBq in the first day from a 10 GBq treatment.

A patient also excretes ^{131}I in urine, with initial concentrations as high as 10^7 Bq/l for an applied treatment of 0.518 GBq (Gründel et al., 2008). We did not attempt to account for the movement of iodine in liquid form in this study. However, some studies (Risher et al., 2004) indicate that as much as 1% of iodine in water will vaporize, thus it could become another atmospheric source term.

A hospital in Richland, Washington, routinely treats hyperthyroidism and thyroid cancer with ^{131}I. Although the number of treatments is not publicized, a study performed for other purposes (Kouzes and Siciliano, 2006; Siciliano, 2004) a number of years ago indicates that on average, the hospital treated one thyroid patient per day in 2001. We examine the possibility whether ^{131}I volatilizing from treated patients could be detected by a system similar to those used in the IMS.

The minimum detectable concentration (MDC) for ^{131}I depends on the sampler, the amount of air that is filtered, and a number of other conditions. Using information from over 25,000 IMS reviewed radionuclide reports from January 2011 through April 2012, 95% of the reported MDC's for ^{131}I were in the range 0.93 to 7.4 μBq/m^3, with a median value of 3.0 μBq/m^3.

Model

Using a source term of 120 MBq/day, we performed atmospheric modeling to determine whether there were locations where air concentrations would exceed the MDC for a sampler. For purposes of this study, we used a MDC of 3.0 μBq/m^3. In the United States, ^{131}I treatments for thyroid cancer do not currently require hospitalization, but for purposes of this study we assume the patient stays near the hospital for 24 hours after the treatment and the iodine they respire is not trapped in a building or filtration system.

Atmospheric transport of ^{131}I was modeled using the Hybrid Single Particle Lagrangian Integrated Trajectory (HYSPLIT) model, parallel version 4.9, maintained by the U.S. National Oceanographic and Atmospheric Administration (Draxler and Hess, 1998; HYSPLIT, 2011). We used three-hour archived meteorological data on a 12-km grid produced for the U.S. National Weather Service's National Centers for Environmental Prediction. The archived meteorological data are available for use in the HYSPLIT model via download from a web server (NAM12, 2012). Because this is an illustrative calculation, we arbitrarily chose to model air movement for the first week of August 2011. Historically, local winds during this month are from the west or southwest.

We used the particle tracking mode of the HYSPLIT code. The particle mode transports a user specified number of representative particles, each released at a specific location and time, and tracks the position of each particle over time. The transport runs were performed on a 168 compute-node Linux cluster. The model used a 0.01° (1.1 km) latitude by 0.01° (0.75 km) longitude transport grid and 40 million particles. The simulated radionuclide activity was injected into the lower 10 meters of the atmospheric column (third story of the hospital) at latitude 46.2814°N and longitude 119.2821°E. Model concentrations at sampling locations were averaged over the bottom 100 meters of the atmospheric column. The top of the 23-layer atmospheric model domain reached 10,000 m above ground level, although the plume does not reach this height in the local region. A dry deposition rate of 1.0 cm/sec was used and radioactive decay was applied. Wet deposition was not used because no precipitation occurred during the modeled time period and there was little cloud cover.

Results

An illustrative ^{131}I plume is shown in Figure II.1 for a source term of 120 MBq per day that is released in hourly increments of 5 MBq. To help understand the spatial scale, it is 200 km from the release location to the city of Spokane (in the upper right of the figure). Wind conditions vary with time, thus the plume changes direction. The typical IMS sampler, such as a Radionuclide Aerosol Sampler/Analyzer (RASA) (Miley et al., 1998) collects air for a 24 hour period, thus the measured concentration is an average over the entire 24-hour period. The illustrative concentrations shown in Figure II.**1** are integrated over a 2-hour time period rather than 24 hours. They are vertically averaged over the lower 100 meters of the modeled air column.

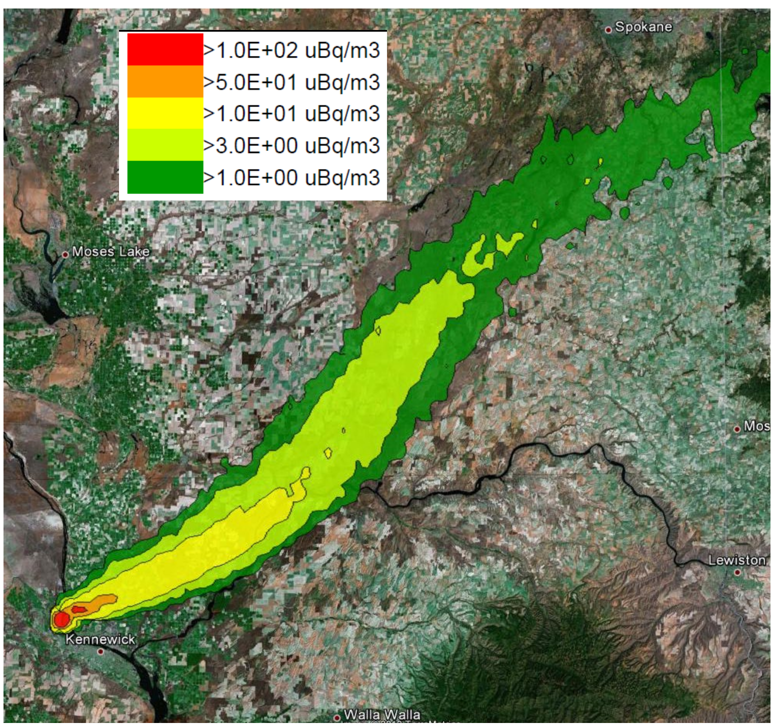

Figure II.1. Illustrative ^{131}I concentrations in surface air (integrated over a 2-hour period) using a source term of 120 MBq per day released in 5 MBq hourly increments.

After integrating the modeled concentrations to 24-hour averages, we examined the resulting concentrations on the 0.01° latitude by 0.01° longitude transport grid. There were 152 grid locations at least 10 km from the source location where the concentrations exceeded 3 μBq/m^3 for at least one of the days. Six of these locations were more than 100 km from the source location, with the furthest one at a distance of 112 km. We also considered the case where the release is an order of magnitude smaller (12 MBq/day). In this case, there were 42 locations where the concentrations exceeded 3 μBq/m^3 for at least one of the days. In this case, the most distant "detection" was 75 km from the hospital.

Discussion

Although this study examined releases from 7 hypothetical patients, the plumes on different days are dominated by the releases from a single patient. These example calculations show that under the correct atmospheric conditions, it is plausible for an IMS sampler to occasionally detect releases from a single patient treated by ^{131}I for thyroid cancer at distances of tens of km.

References

Abu-Khaled, Y.S., Sandouqa, A.S., Haddadin, I.M., 2009. Radiation exposure from radioactive iodine 131I in and surrounding the patients' room. Radiat. Prot. Dosimet. 135(1), 64-68. doi:10.1093/rpd/ncp093

Biegalski, S.R., Bowyer, T.W., Eslinger, P.W., Friese, J.A., Greenwood, L.R., Haas, D.A., Hayes, J.C., Hoffman, I., Keillor, M., Miley, H.S., Moring, M., 2012. Analysis of Data from Sensitive U.S. Monitoring Stations for the Fukushima Daiichi Nuclear Reactor Accident. J. Environ. Radioact. 114, 15-21. doi:10.1016/j.jenvrad.2011.11.007

CNEA. 2012. Centro Atomico Ezeiza. Accessed on April 24, 2012, at http://caebis.cnea.gov.ar/

CTBT. 1996. Text of the Comprehensive Nuclear-Test-Ban Treaty. United Nations Office for Disarmament Affairs (UNODA), Status of Multilateral Arms Regulation and Disarmament Agreements, CTBT. Accessed on October 7, 2011, at http://disarmament.un.org/TreatyStatus.nsf

CTBTO. 2011. CTBTO Preparatory Commission Web Page. Accessed on September 24, 2011, at http://www.ctbto.org/

Draxler, R.R., Hess, G.D., 1998. An overview of the HYSPLIT_4 modeling system of trajectories, dispersion, and deposition. Aust. Meteor. Mag. 47, 295-308,

Gründel, M., Kopka, B., Schulz, R., 2008. 131I exhalation by patients undergoing therapy of thyroid diseases. Radiat. Prot. Dosimet. 129(4), 435-438. doi:10.1093/rpd/ncm459

HYSPLIT. 2011. Air Resources Laboratory HYSPLIT Model. Accessed on October 3, 2011, at http://www.arl.noaa.gov/documents/Summaries/HYSPLIT_FINAL.pdf (last updated March 2011).

IAEA. 2011. Source of Iodine-131 in Europe Identified. International Atomic Energy Agency. Accessed on April 24, 2012, at http://www.iaea.org/newscenter/pressreleases/2011/prn201127.html

JINR. 2012. Joint Institute for Nuclear Research. Accessed on April 24, 2012, at http://www.jinr.ru/

Kouzes, R.T., Siciliano, E.R., 2006. The response of radiation portal monitors to medical radionuclides at border crossings. Radiat. Measur. 41(5), 499-512. doi:10.1016/j.radmeas.2005.10.005

Li, C., Sadi, B., Wyatt, H., Bugden, M., Wilkinson, D., Cornett, J., Kramer, G.H., 2012. Excretion of volatile 131I from rats following administration of Na131I or MIBG-131I. Radiat. Prot. Dosimet. 148(2), 143-148. doi:10.1093/rpd/ncr008

Matthews, K.M., 2009. Spurious Iodine-131 detections at remote IMS radionuclide stations (Poster RN-06/D), ISS09 (International Scientific Studies) Conference, June 10-12, 2009. CTBTO Preparatory Commission, Vienna, Austria, http://www.ctbto.org/fileadmin/user_upload/ISS_2009/Poster/RN-06D%20%28New%20Zealand%29%20-%20Murray_Matthews.pdf

Matthews, K.M., Saey, P.R.J., Bowyer, T.W., Vandergrift, G., Ramamoorthy, N., Cutler, C., Ponsard, B., Mikolajczak, R., Tsipenyuk, Y.M., Solin, L.M., Fisher, D., Ungar, K., Dolinar, G., Higgy, R., Schraick, I., et al., 2010. Workshop on Signatures of Medical and Industrial Isotope Production - A Review., Pacific Northwest National Laboratory, Richland, Washington, http://wosmip.pnnl.gov/WOSMIPReviewPNNL-19294.pdf

Miley, H., Bowyer, S., Hubbard, C., McKinnon, A., Perkins, R., Thompson, R., Warner, R., 1998. A description of the DOE Radionuclide Aerosol Sampler/Analyzer for the Comprehensive Test Ban Treaty. J Radioanal Nucl Chem 235(1-2), 83-87. doi:10.1007/BF02385942

NAM12. 2012. Downloadable North American data assimilation system information archive. Air Resources Laboratory, National Oceanic and Atmospheric Administration. Accessed on April 24, 2012, at ftp://arlftp.arlhq.noaa.gov/pub/archives/nam12/

NRU. 2012. The NRU Reactor. Accessed on April 24, 2012, at http://www.nrureactor.ca/

Risher, J., Diamond, G., Swarts, S.G., Amata, R., 2004. Toxological Profile for Iodine, U.S. Department of Health and Human Services, Agency for Toxic Substances and Disease Registry, Atlanta, Georgia, http://www.atsdr.cdc.gov/toxprofiles/tp158.pdf

Siciliano, E.R., 2004. Medical Radioisotope Data Survey: 2002 Preliminary Results, PNNL-14882, Pacific Northwest National Laboratory, Richland, Washington, http://www.pnl.gov/main/publications/external/technical_reports/PNNL-14882.pdf

PNNL-SA-32446

Pacific Northwest National Laboratory

902 Battelle Boulevard
P.O. Box 999
Richland, WA 99354
1-888-375-PNNL (7665)

www.pnnl.gov